EPJ Web of Conferences **83**, 02014 (2015)
DOI: 10.1051/epjconf/20158302014

Rotational disorder in lithium borohydride

Arndt Remhof[1,a], Yigang Yan[1], Jan Peter Embs[2], Victoria Garcia Sakai[3], Angeloclaudio Nale[4], Petra de Jongh[4], Zbigniew Łodziana[5] and Andreas Züttel[1,6]

[1]Hydrogen and Energy, Empa, Swiss Federal Laboratories for Materials Science and Research, Dübendorf, Switzerland
[2]Laboratory for Neutron Scattering, Paul Scherrer Institut, Villigen, Switzerland
[3]ISIS Facility, Rutherford Appleton Laboratory, Chilton, Didcot, Oxon, UK
[4]Inorganic Chemistry and Catalysis, Debye Institute for Nanomaterials Science, Utrecht University, The Netherlands
[5]Institute of Nuclear Physics, Polish Academy of Sciences, Kraków, Poland
[6]École Polytechnique Fédérale de Lausanne (EPFL), Institut des Sciences et Ingénierie Chimique, Lausanne, Switzerland

Abstract. $LiBH_4$ has been discussed as a promising hydrogen storage material and as a solid-state electrolyte in lithium-ion batteries. It contains 18.5 wt% hydrogen and undergoes a structural phase transition at 381 K which is associated with a large increase in rotational disorder of the $[BH_4]^-$ anion and the increase of $[Li]^+$ conductivity by three orders of magnitude. We investigated the $[BH_4]^-$ anion dynamic in bulk $LiBH_4$, in $LiBH_4$-LiI solid solutions and in nano-confined $LiBH_4$ by quasielastic neutron scattering, complemented by DFT calculations. In all cases the H-dynamics is dominated by thermally activated rotational jumps of the $[BH_4]^-$ anion in the terahertz range. The addition of LiI as well as nano-confinement favours the disordered high temperature phase and lowers the phase transition below room temperatures. The results are discussed on the basis of first principles calculations and in relation to ionic conductivity of $[Li]^+$.

1. Introduction

Lithium borohydride ($LiBH_4$) is an ionic crystal consisting of negatively charged $[BH_4]^-$ ions and positively charged $[Li]^+$ ions [1]. Within the $[BH_4]^-$ unit the hydrogen atoms surround the boron in a tetrahedral configuration. At $T_c = 381$ K $LiBH_4$ undergoes a first order structural phase transition from an orthorhombic low-temperature (LT) structure to a hexagonal high-temperature (HT) structure. [2,3]. Apart from its classical application as a reducing agent or as a starting compound for the synthesis of organometallic derivatives, the light-weight $LiBH_4$, together with its chemical relatives such as $NaBH_4$ have recently been discussed as synthetic fuels either in the direct borohydride fuel cell [4] or as hydrogen storage materials for mobile applications [5,6]. In addition, owing to its high lithium ion conductivity, $LiBH_4$ and related compounds are considered as potential solid-state electrolytes for lithium-ion batteries [7,8].

Apart from being an ionic conductor, the HT phase is associated with dynamical disorder of the $[BH_4]^-$ anions, which undergo reorientational jumps in the terahertz range. Strong lattice anharmonicities are present in this phase [9,10]. In many cases, the rotational motion of the anion seems to be a prerequisite for the fast cation mobility and thereby for the ionic conductivity.

In the present study we review the rotational motion of the $[BH_4]^-$ tetrahedra in bulk and nanoconfined $LiBH_4$ as well as in $LiBH_4$-LiI solid solutions. In a combined experimental and theoretical approach, we discuss the origin of disorder in bulk $LiBH_4$ and the effect of imposed disorder either by halide additives or by nano-confinement. Finally, we discuss the relation between the orientational disorder and ion conductivity.

2. Bulk $LiBH_4$

Figure 1 displays QENS spectra of bulk $Li^{11}BH_4$ recorded at 320 K (LT phase) at the time-of flight spectrometer "IRIS" at the ISIS facility of the Rutherford Appleton Laboratory in Didcot, UK [11].

Incident neutrons with a wavelength of $\lambda = 6.66$ Å and an energy resolution of 17.5μ eV were chosen. Details of the instrumental settings and the data acquisition are described in ref. [12]. The scattered intensity $S(Q,\omega)$ is expressed as function of energy transfer $\Delta E = \hbar\omega = E_i - E_f$, and of momentum transfer $\hbar Q = \hbar k_i - \hbar k_f$. Thereby E_i and E_f are the incident and scattered neutron energies and k_i and k_f, are the incident and scattered wave vectors, respectively. Figure 1 displays a series of spectra for $0.5\,\text{Å}^{-1} < Q < 2.15\,\text{Å}^{-1}$, recorded at 320 K, i. e. within the low temperature phase. The QENS spectra were modelled by using (i) a resolution limited elastic peak using a Gaussian line shape of width w_{el} and an integrated area I_{el}, and (ii) a quasielastic component using a Lorentzian line shape of width w_{qe} and integrated area I_{qe}. At any given temperature, the quasielastic broadening is independent of Q, as expected for the localized rotational $[BH_4]^-$ jump diffusion. The broadening follows the Arrhenius law, indicative of a thermally activated process [12,13].

Inelastic fixed window scans measured with high-resolution back-scattering spectroscopy revealed the

[a] Corresponding author: arndt.remhof@empa.ch

presence of two kinds of rotational motion at low temperatures with activation energies of 162 meV and 232 meV [12], respectively, in accordance with NMR measurements [14,15]. The dominating motion could be identified as a three-fold jump rotation of the $[BH_4]^-$ anion around the c3 axis [12,13]. In the high temperature phase the $[BH_4]^-$ anion undergoes rapid reorientational jumps, accompanied by quasi-free, trigonal-axis rotation of three borohydride H atoms [16]. The dynamic behaviour of $LiBH_4$ has been interpreted by DFT calculations on the basis of potential energy landscapes of $[BH_4]^-$ rotation about its high symmetry axes. In the low temperature phase, the potential energy surface is characterized by distinct energy minima, separated by energy barriers. Consequently, the orientation of a $[BH_4]^-$ unit is fairly localized and coincide with the equivalent orientations of the $[BH_4]^-$ unit. In the high temperature phase the potential energy landscape is significantly different. The phase transition changes the symmetry and lowers the barriers. The potential seen by rotating $[BH_4]^-$ ion is very shallow when compared to LT phase, and localized minima are not present. As a result, the jump frequencies increase, leading to rotational disorder [17]. The distribution of hydrogen around boron atoms related to the crystal structure is discussed below in view of *ab initio* molecular dynamics simulations.

3. $LiBH_4$-LiI solid solutions

Disorder can be achieved by ion substitution. One of the most studied examples in this respect are $LiBH_4$-LiI solid solutions, in which $[BH_4]^-$ ions are randomly replaced by $[I]^-$ ions [18]. As a result, the disordered phase is favoured and the phase transition is shifted to lower temperatures.

The formation of the solid solution and its temperature characteristics can be studied by means of elastic fixed window scans (EFWS). Figure 2 displays the corresponding EFWS, measured at IRIS, summed over the whole Q-range.

For the bulk sample, the hydrogen dynamics matches the time window of the IRIS spectrometer and a quasielastic broadening is observed between $240\,K < T < 360\,K$ [12]. The phase transition can be seen as the intensity step at 390 K. At any given temperature, the elastically scattered intensity of the $Li^{11}BH_4 : LiI$ (4 : 1) solid solution lies below the intensity of the bulk material. The hydrogen dynamics enters the time window of the instrument earlier, i.e. the deviation from the Debye Waller behaviour occurs at lower temperature. The phase transition can be seen at 340 K. Upon cooling, a hysteretic behaviour is observed. The sample follows the high temperature behaviour and the hydrogen dynamics matches the time window between 220 K and 150 K. The hysteresis is only observed in the first temperature cycle. In the subsequent cycles the heating as well as the cooling follow the first cooling curve. L. Rude et al. [18] observed that $LiBH_4$-LiI solid solutions can be achieved either by high energy ball milling (as in the present case) or by heat treatment. We attribute the hysteresis to an initially incomplete intermixing of $LiBH_4$ and LiI. Above the phase transition, due to the enhanced ion mobility, the two constituents completely intermix and no phase

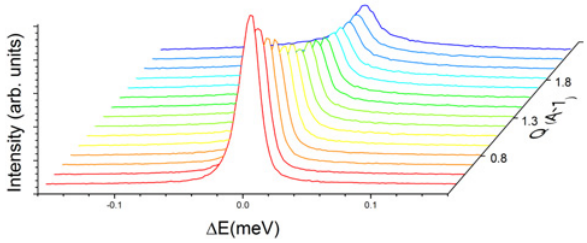

Figure 1. QENS spectra of $LiBH_4$, recorded at 320 K at IRIS.

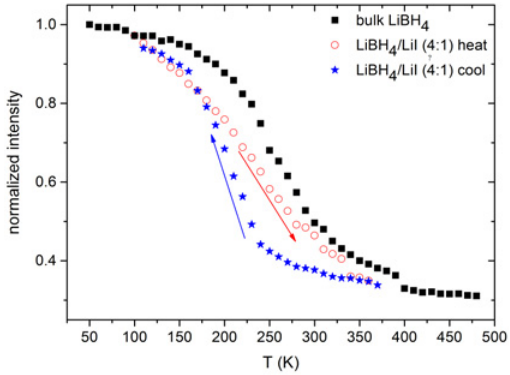

Figure 2. Elastic fixed window scan of $LiBH_4$ (black) and a $LiBH_4$: LiI (4:1) solid solution recorded at IRIS.

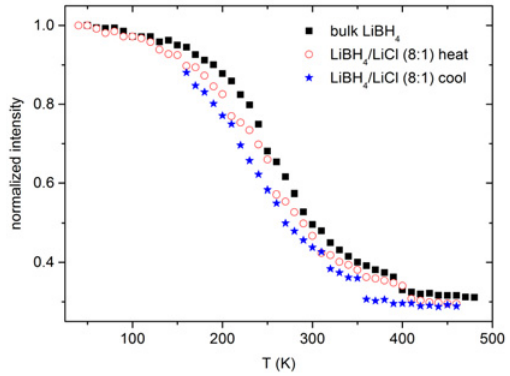

Figure 3. Elastic fixed window scan of $LiBH_4$ (black) and a $LiBH_4$- LiCl (8:1) solid solution recorded at IRIS.

transition is observed. Detailed studies of the T and Q dependence of the quasielastic broadening of $LiBH_4$-LiI solid solutions reveal indeed rapid rotational jump diffusion of the $[BH_4]^-$ anion, similar to the behaviour of the bulk HT $LiBH_4$ phase [9,10]. The $LiBH_4$- LiI solid solutions show lower activation energies and shorter dwell times as the $[I]^-$ concentration increases. At room temperature, the jump frequency is in the terahertz regime with activation energies in the order of 50 meV, well below the value of bulk $LiBH_4$ at RT and even lower than the activation energy for $[BH_4]^-$ rotation in the HT-phase. Thus, the addition of $[I]^-$ has qualitatively the same effect as a temperature increase. [19,20].

A similar behaviour can be observed in $LiBH_4$-LiCl solid solutions. However, due to the smaller size of the $[Cl]^-$ compared to the $[I]^-$, the effect is less pronounced. Figure 3 displays the EFWS of bulk $Li^{11}BH_4$ and of the $LiBH_4$-LiCl (8:1) solid solution as an example.

4. Nano-confined $LiBH_4$

Confinement of $LiBH_4$ in small pores, for instance in a porous carbon material, can increase hydrogen release and uptake kinetics [21]. In combination with a small amount of additives such as Ni the reversibility can be enhanced significantly [22]. The dynamical properties of $LiBH_4$ confined in high surface area graphite (HSAG) were investigated by inelastic and quasielastic neutron scattering. Thereby, the loss in crystallographic order and the suppression of the phase transition was observed [23]. With respect to dynamical properties, two different $[BH_4]^-$ populations were distinguished. One showing the signature of the HT phase, i.e. an elastic intensity approaching zero at higher Q and a low activation energy of 83 meV(= 8 kJ/mol). The other half was immobile within the temporal resolution of the instrument [23]. N. Verdal et al. identified the two populations as more rapidly reorienting $[BH_4]^-$ anions in the vicinity of the pore surfaces and more slowly reorienting $[BH_4]^-$ anions in the interior of the pores [24].

The origin of the modified physical properties due to nanoconfinement may be (i) a finite size effect due to the confined space (ii) strain effects due to different thermal expansion coefficients, (iii) an interface effect due to the interaction of the confined material with the host or (iv) a combination of all. To separate the effect of the host, we compared two chemically different hosts, carbon aerogel (CA) and mesoporous silica (SBA15). The pores in these hosts are mono-disperse and their size can be tuned over a wide range. Pore sizes of 12.1 and 13 nm were chosen for the silica and for the CA, respectively.

Figure 4 shows close-ups of the time of-flight spectra, i.e. the scattered intensity (summed over all detectors) as function of neutron's time-of-flight for (a) bulk $Li^{11}BH_4$, (b) 22.3 wt% $Li^{11}BH_4$ in CA with 13 nm sized pores, and (c) 28.4 wt% $Li^{11}BH_4$ in SBA15 with 12 nm pore size. The spectra were recorded at the time-of-flight spectrometer "FOCUS" located at the Paul Scherrer Institute in Villigen, Switzerland [25]. In this case incident neutrons with a wavelength of 4 Å were used and the energy resolution was 200 μeV. The TOF spectra allow a qualitative comparison of the three samples. In close-up (a), the different shapes of the spectra in the LT and the HT phase as well as the temperature dependence of the line broadening for the bulk sample is clearly visible. For the bulk sample (panel a) the phase transition is accompanied by a sudden decrease of the elastically scattered intensity (around 3.1 ms) and an increase of the inelastically scattered intensity. A HSAG sample with a typical pore size of 2–3 nm, containing 15 wt% $LiBH_4$, does not show a phase transition, the spectra vary continuously with temperature [23]. In the present CA and SBA15 samples, an intermediate performance is observed, where characteristics of the nanoconfined behaviour coexist with bulk behaviour. The $LiBH_4$ phase transition is still present but less pronounced.

In the following, we discuss the intensity changes at flight times between 2.5 and 2.75 ms, i.e. beside the elastic line. For the bulk sample, the intensity increases by a factor of 3 between the scans recorded at 360 K and 390 K, respectively. For $LiBH_4$ confined in CA (panel b), the intensity increases by less than a factor

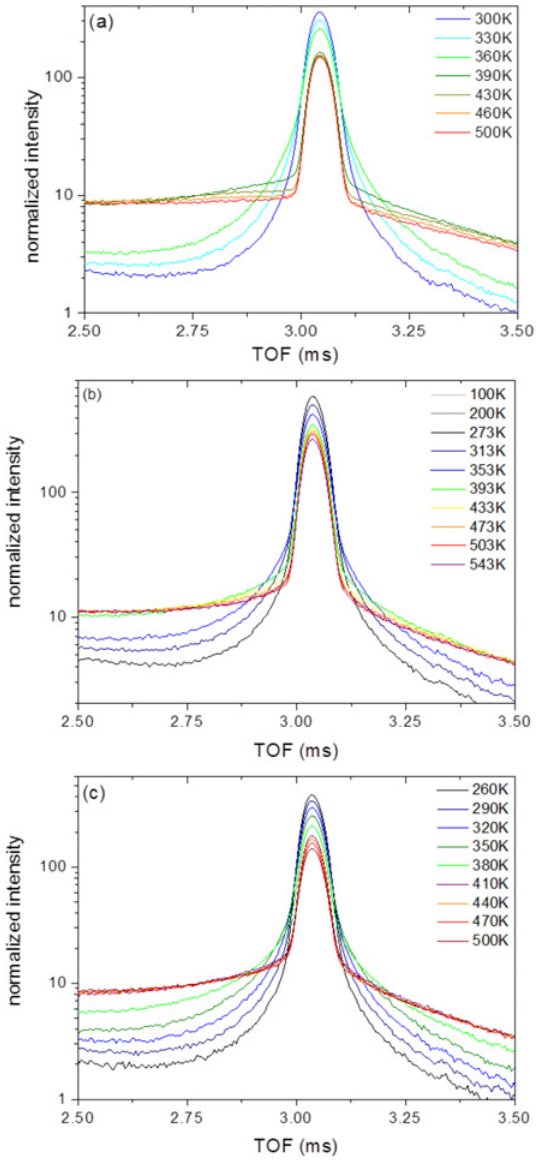

Figure 4. TOF spectra of (a) bulk LiBH4, (b) 22.3 wt% $LiBH_4$ in CA with 13 nm sized pores, and (c) 28.4 wt% $LiBH_4$ in SBA15 with 12 nm pore size. The spectra were recorded at FOCUS.

of two, even though the temperature difference between the scans is larger. For the last sample, $LiBH_4$ in SBA 15 (panel c), the intensity increase is even lower. Also within the HT phase, the samples behave differently. In the bulk HT phase, the spectra vary with temperature. This temperature dependence is less pronounced in the nanoconfined samples. Thereby the deviation from the bulk behaviour is strongest in the SBA15 sample where the spectra recorded at high temperatures almost coincide.

Generally, as in the case of $LiBH_4$ supported in HSAG [23], confinement of $LiBH_4$ in CA and in SBA15 reduces the phase transition temperature and lowers the activation energy. In all cases the effects of confinement increase with decreasing pore-size. The carbon samples thereby show a more "bulk like" behavior, even with lower filling fraction. This behavior is attributed to the lower surface energy of carbon [26]. The origin of the modified physical properties due to nanoconfinement is obviously a combination of

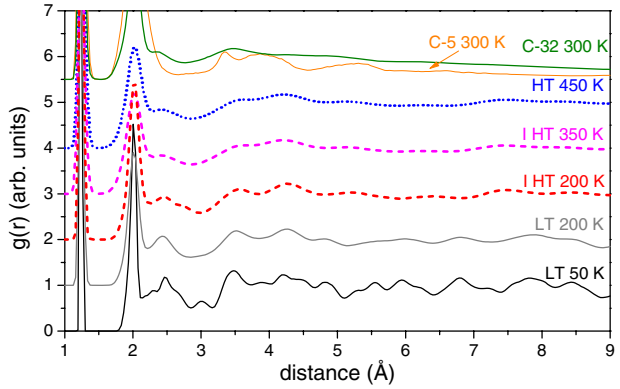

Figure 5. The radial distribution function (RDF) for the bulk LiBH4, at 50 K (LT 50 K), 200 K (LT 200 K) and 450 K (HT 450 K); for the 25% iodine doped structure at 200 K (I HT 200 K), 350 K (I HT 350 K). The RDF calculated at T = 300 K for nano-clusters of 32 (C-32 300 K) and 5 (C-5 300 K) formula units are shown in the upper part.

several effects including finite size effects and interface effects.

5. Radial distribution functions

In order to interpret the type of behavior observed in pure, I-doped and nanoconfined $LiBH_4$ a series of *ab initio* molecular dynamics simulations (MD) were carried out, for details see [27]. The atomic structure of any solid can be described by means of the radial distribution function (RDF), describing the probability of finding a particle (atom) at a distance of r away from the origin. The RDF was calculated for the low and high temperature phases of pure $LiBH_4$, for iodine doped phase and for nano-clusters, respectively. The RDF was calculated for temperatures below the bulk phase transition temperature ($T < T_c$), except the reference calculations for HT phase at T = 450 K.

Interestingly, for linear clusters the separation between boron and lithium is smaller than in the bulk, and the corresponding peak merges with the peak of the H-H distance. For 3-dimensional cluster however, the local cation/anion ordering resembles RDF of the high temperature phase. In the $LiBH_4$-LiI system at T = 350 K the local distribution of atoms resembles this of the HT phase at T = 450 K, while at T = 200 K similarity to the LT phase can be observed in Fig. 5. These results indicate the similarity of the local structure around atoms in the HT phase at T = 450 K, $LiBH_4$- LiI at T = 350 K, and small $LiBH_4$ cluster of 32 formula units at T = 300 K.

6. Hydrogen distribution within $[BH_4]$

The hydrogen distribution, around the central boron of each anion, i.e. the probability of finding a hydrogen atom on a sphere with radius 1.2 Å, the B-H distance, provides information about the rotational motion of anions. The distribution was calculated for the bulk systems by projection of hydrogen positions on the basal plane along the c lattice direction. For each projection the boron atom was placed at the origin of the plane. The probability distribution is presented in Fig. 6. For the pure $LiBH_4$ at T = 200 K librational motion is clearly visible, however the distribution of the probability consist of four separated regions indicating that each H atom oscillates around its equilibrium lattice site. For the iodine doped system at the same temperature a finite probability of hydrogen being located between the equilibrium positions can be observed, Fig. 6 (middle panel).

These finite probability regions link the equilibrium hydrogen positions and correspond to the re-orientational jumps of $[BH_4]^-$ anions at T = 200 K. In the high temperature phase the probability of finding a hydrogen atom outside of the equilibrium basins is larger than for $LiBH_4$-LiI. This is an indication of quasi-free rotational motion.

7. Discussion and summary

The hexagonal high temperature phase of $LiBH_4$ is characterized by dynamic disorder, evidenced by fast rotational jumps of the $[BH_4]^-$ anion in the terahertz regime as well as by translational mobility of the $[Li]^+$ cation, leading to high ionic conductivity ($\sigma \sim 10^{-3}$ S/cm) [7,8]. Disorder can be imposed below the phase transition temperature by ion substitution or by nano-confinement. In both cases the $LiBH_4$ adopts a high temperature like phase at room temperature or even at cryogenic temperatures. The radial distribution function for $LiBH_4$-LiI and of $LiBH_4$ nano-clusters at $T < 300$ K resembles the one of the bulk HT phase. The long range ordering of atoms separated by more than 3 Å is significantly hampered with respect to the LT phase. However, the local structure of the $[BH_4]^-$ anion remains intact in all structures. Experimentally as well as theoretically the orientational disorder of the anion is accompanied by high cation diffusivity. The concurrent occurrence of high $[Li]^+$ conduction and rotational mobility of the counter ion is not a singular case. Also Li_2SO_4 and Li_3PO_4, which possess complex anions, undergo structural phase transitions and they are good ionic conductors in their respective HT phases. Thereby, the rotation of the anion is believed to support the cation diffusion by the so-called "paddle wheel mechanism" [28].

At present there is no direct evidence for a "paddle wheel" mechanism in $LiBH_4$, where the rotating anions shovels the cations, or for a "revolving door" mechanism, where the moving cations drive the anions. In fact, there is no evidence for a causal connection between the ion conductivity and the anion rotation in $LiBH_4$ [29]. The rotational disorder of $[BH_4]^-$ anions is evidenced by the probability of hydrogen distribution around the central boron atom calculated by *ab initio* MD method. In the low temperature phase hydrogen is localized, and the span of the probability distribution around each equilibrium position corresponds to the amplitude of librational and bending modes of anions. In the HT phase the equilibrium positions are linked by finite probability regions, which originate from successive rotational jumps of hydrogen. Similar behaviour is evidenced for iodine doped phase even at T = 200 K. The increased ion conductivity in the $[I]^-$ doped samples suggest that $[Li]^+$ and $[BH_4]^-$ move jointly together: A $[Li]^+$ jump causes the neighbouring

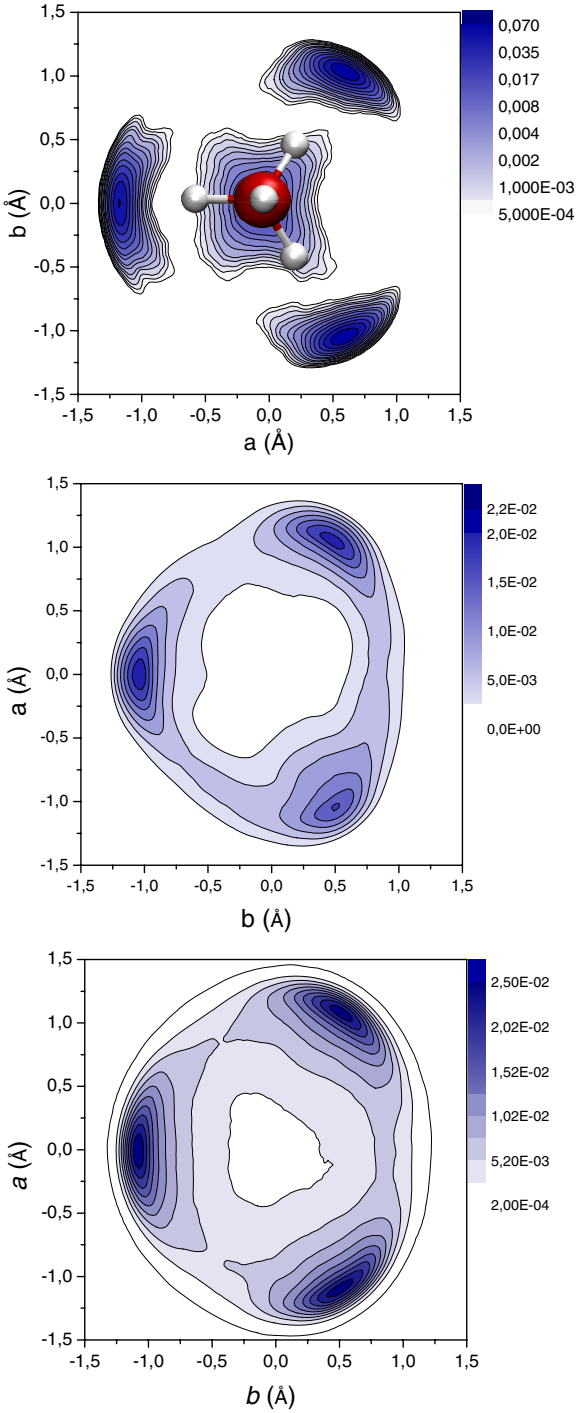

Figure 6. The probability distribution for hydrogen location around the central boron atom of $[BH_4]^-$ anions for the LT phase at T = 200 K – top; for I doped phase at T = 200 K middle, and for HT phase at T = 400 K, bottom panel. The schematic arrangement of the ion is shown in for the LT phase, with red sphere for boron, white ones for hydrogen.

$[BH_4]^-$ to adjust their orientation accordingly. In the low temperature phase, the immobile, non-spherical $[BH_4]^-$ hinder the $[Li]^+$ mobility. In case of the spherical $[I]^-$, the orientation of the anion does not play a role [19]. However, in view of potential applications, that rely on $[Li]^+$ ion conductivity, nanoconfinement and halide doping are promising routes to increase the ion conductivity at room temperature.

This experimental work is based on experiments performed at the Swiss spallation neutron source SINQ, Paul Scherrer Institute, Villigen, Switzerland and at the ISIS facility of the Rutherford Appleton Laboratories in Didcot, UK.

Financial support by a grant from Switzerland through the Swiss Contribution to the enlarged European Union is gratefully acknowledged. We also acknowledge the MP1103 COST Action "Nanostructured materials for solid-state hydrogen storage". Z. L. acknowledges CPU allocation at PL-Grid Infrastructure.

References

[1] F. Buchter, Z. Lodziana, A. Remhof, Ph. Mauron, O. Friedrichs, A. Borgschulte, A. Züttel, Y. Filinchuk, L. Platinus, Phys. Rev. B **83**, 064107 (2011)
[2] J. Ph. Soulié, G. Renaudin, R. Černý, K Yvon, J. Alloys Compd. **346**, 200 (2002)
[3] M. R. Hartman, J. J. Rush, T. C. Udovic, R. C. Bowman, S. J. Hwang, J. Solid State Chem. **180**, 1298 (2007)
[4] B. H. Liu, Z. P. Li, J. Power Sources **187**, 291 (2009)
[5] A. Züttel, A. Borgschulte, S. I. Orimo, Scr. Mater. **56**, 823 (2007)
[6] M. B. Ley, L. H. Jepsen, Y.-S. Lee, Y. W. Cho, J. M. Bellosta von Colbe, M. Dornheim, M. Rokni,J. O. Jensen, M. Sloth, Y. Filinchuk, J. E. Jø, F. Besenbacher, T. R. Jensen, Materials Today **17**, 122 (2014)
[7] M. Matsuo, S. I. Orimo, Adv. Energy Mat. **1**, 161 (2011)
[8] A. Unemoto, M. Matsuo, S.-i. Orimo, Adv. Funct. Mater. **24**, 2267 (2014)
[9] S. K. Callear, E. A. Nickels, M. O. Jones, M. Matsuo, S. I. Orimo, P. P. Edwards, W. I. F. David, J. Mater. Sci. **46**, 566 (2011)
[10] F. Buchter, Z. Lodziana, Ph. Mauron, A. Remhof, O. Friedrichs, A. Borgschulte, A. Züttel, D. Sheptyakov, T. Strässle, A. J. Ramirez-Cuesta, Phys. Rev. B **78**, 094302 (2008)
[11] C. J. Carlile and M. A. Adams, Physica B **182**, 431 (1992)
[12] A. Remhof, A. Züttel, A. J. Ramirez-Cuesta, V. García-Sakai, B. Frick, Chem. Phys. **427**, 18 (2013)
[13] A. Remhof, Z. Lodziana, P. Martelli, O. Friedrichs, A. Züttel, A. V. Skripov, J. P. Embs, T. Strässle, Phys. Rev. B **81**, 214304 (2010)
[14] A.V. Skripov, A.V. Soloninin, Y. Filinchuk, D. Chernyshov, J. Phys. Chem. C **112**, 18701 (2008)
[15] K. Jimura, S. Hayashi, J. Phys. Chem. C 116, **4883** (2012)
[16] N. Verdal, T. J. Udovic, J. J. Rush, J. Phys. Chem. C, **116**, 1614 (2012)
[17] F. Buchter, Z. Łodziana, Ph. Mauron, A. Remhof, O. Friedrichs, A. Borgschulte, A. Züttel, D. Sheptyakov, T. Strässle, A. J. Ramirez-Cuesta, Phys. Rev. B **78**, 094302 (2008)
[18] L. H. Rude, E. Groppo, L. M. Arnbjerg, D. B. Ravnsbæk, R. A. Malmkjær, Y. Filinchuk M. Baricco, F. Besenbacher, T. R. Jensen, J. Alloys Compd., **509**, 8299 (2011)

[19] P. Martelli, A. Remhof, A. Borgschulte, R. Ackermann, T. Strässle, J. P. Embs, M. Ernst, M. Matsuo, S.-I. Orimo, Andreas Züttel, J. Phys. Chem. A **115**, 5329 (2011)
[20] N. Verdal, T. J. Udovic, J. J. Rush, H. Wu, A. V. Skripov, J. Phys. Chem. C **117**, 12010, (2013)
[21] A. F. Gross, J. J. Vajo, S. L. van Atta, G. L. Olson, J. Phys. Chem. C **112**, 5651, (2008)
[22] P. Ngene, M. van Zwienen, P.E. de Jongh, Chem. Comm. **46**, 8201, (2010)
[23] A. Remhof, P. Mauron, A. Züttel, J. P. Embs, Z. Lodziana, A. J. Ramirez-Cuesta, P. Ngene, P. de Jongh, J. Phys. Chem. C, **117**, 3789 (2013)
[24] N. Verdal, T. J. Udovic, J. J. Rush, X. Liu, E. H. Majzoub, J. J. Vajo, A. F. Gross, J. Phys. Chem. C, **117**, 17983 (2013)
[25] S. Janssen, J. Mesot, L. Holitzner, A. Furrer, R. Hempelmann, Phys. B, **234–236**, 1174, (1997)
[26] S. Suwarno, A. Nale, A. Remhof, T. Eggenhuisen, P. Ngene, P.E. de Jongh, submitted
[27] Z. Lodziana, P. Bloński, Int. J. Hydrogen Energy, **39**, 9842 (2014)
[28] A. Lunden, Z. Naturforsch., A: Phys. Sci., **50**, 1067 (1995)
[29] A. Borgschulte, A. Jain, A. J. Ramirez-Cuesta, P. Martelli, A. Remhof, O. Friedrichs, R. Gremaud, A. Züttel, Faraday Discuss., **151**, 213 (2011)